Bluetongue virus VP6 and genomic RNA interaction is essential for genome packaging

Po-Yu Sung[1], Robert Vaughan[2], Shah Kamranur Rahman[1], Guanghui Yi[3], Adeline Kerviel[1], C. Cheng Kao[3] and Polly Roy[1,*]

1. Faculty of Infectious and Tropical Diseases, London School of Hygiene and Tropical Medicine, London, WC1E 7HT, United Kingdom
2. Biotechnology Program, Indiana University Bloomington. Bloomington IN, 47401, United States
3. Department of Molecular & Cellular Biochemistry, Indiana University Bloomington. Bloomington IN , 47401, United States

* To whom correspondence should be addressed. Tel: +44 (0)20 7927 2324; Email: polly.roy@lshtm.ac.uk

Running Title: Bluetongue virus VP6 packages RNA

Word Count: Abstract 210
Word Count: Text 5473

ABSTRACT

The genomes of the *Reoviridae*, including the animal pathogen Bluetongue virus (BTV), are multi-segmented double-stranded (ds) RNA. During replication, single-stranded (ss) positive-sense RNA segments are packaged into the assembling virus capsid, triggering genomic dsRNA synthesis. However, exactly how this packaging event occurs is not clear. A minor capsid protein VP6, unique for the orbiviruses, has been proposed to be involved in the RNA packaging process. In this study, we sought to characterize the RNA binding activity of VP6 and its functional relevance. A novel proteomic approach was utilized to map the ss/dsRNA binding sites of a purified recombinant protein and the genomic dsRNA binding sites of the capsid-associated VP6. The data revealed each VP6 has multiple distinct RNA binding regions and only one region is shared between recombinant and capsid-associated VP6. A combination of targeted mutagenesis and reverse genetics identified the RNA-binding region that is essential for virus replication. Using an *in vitro* RNA-binding competition assay, a unique *cell-free* assembly assay and an *in vivo* single cycle replication assay, it was possible to identify a motif within the shared binding region that binds BTV ssRNA preferentially consistent with specific RNA recruitment during capsid assembly. These data highlight the critical roles this unique protein plays in orbivirus genome packaging and replication.

Importance

Genome packaging is a critical stage during virus replication. For virus with segmented genome, the genome segments need to be correctly packaged into a newly formed capsid. However, the detailed mechanism of this packaging is unclear. Here we focus on VP6, a minor viral protein of Bluetongue virus, which is critical for genome packaging. We use multiple approaches including a robust RNA-protein finger-printing assay, which map the ssRNA binding sites of recombinant VP6 and the genomic dsRNA binding sites of the capsid-associated VP6. Together with virological and biochemical methods, within VP6, we for the first time identify the viral RNA packaging motif of a segmented dsRNA virus.

Keywords: **Genome packaging/RNA-protein interaction/dsRNA virus**

INTRODUCTION

Bluetongue virus (BTV) is an important animal pathogen and the prototype of the *Orbivirus*, a genus of the *Reoviridae* family. The BTV particle has two capsids, an outer capsid and an inner capsid, the latter of which is also called the core. The outer capsid contains proteins VP2 and VP5 to facilitate virus entry through the cellular membrane and the release of the core into the cytoplasm. The icosahedral-shaped core is principally comprised of two proteins, VP7 and VP3, which are arranged in two layers. The VP3 encloses the viral genome of ten double-stranded RNA (dsRNA) segments (S1-S10). In addition, the core contains three minor proteins: the polymerase (VP1), the capping enzyme (VP4), and VP6, an essential structural protein of 36 kDa with RNA binding and ATP binding activity. VP6 is unique among the *Orbivirus* genus within the *Reoviridae* family.

Upon entry, core particles become transcriptionally active, producing and extruding single-stranded positive-sense RNAs (ssRNA) through the local channels at the five-fold axis, without further disassembly. These ssRNAs then act both as mRNAs for viral protein synthesis, and as templates for nascent genomic RNA synthesis. Our current understanding is that the newly synthesised 10 ssRNA segments are first combined via specific intersegment RNA-RNA interactions to form RNA complexes of all 10 segments. The RNA complexes of 10 segments are then packaged together with VP1, VP4 and VP6, into the assembling VP3 capsid layer (1-4). Genomic dsRNA molecules are subsequently synthesized within this assembled particle (known as the 'subcore'), prior to encapsidation by the VP7 layer, leading to a robust core particle formation (5).

VP1 polymerase and capping enzyme VP4 are likely to be located beneath the VP3 layer at or near the five-fold axis of icosahedral symmetry to facilitate the release of newly synthesised transcripts (6, 7). However, the exact location of VP6 is not yet clear, although VP6 has specific binding affinity for VP3 and this interaction has been shown to be important for viral ssRNA packaging and replication (8). Using reverse genetics (RG), we have shown that VP6 is essential for BTV replication and that modified BTV strains lacking VP6 do not replicate in normal cells but only in a VP6 helper cell line (9). Further, when VP6-deficient viruses were grown in VP6 helper cells and used for infection of normal cells, viral proteins are synthesized and assemble as empty particles without the viral genome. This data suggests that VP6 may be responsible for genome packaging (10, 11).

The smallest core associated protein, VP6 (328 aa), has high binding affinity for both ssRNA and dsRNA species, suggesting that it is closely associated with the viral genome (12, 13). VP6 was previously suggested to be an RNA helicase, despite poor homology with known

helicases (14). Current hypothesis is that VP6 assists in ssRNA packaging into the viral core through the interaction with VP3 (1, 8, 15). However, questions concerning the definition of the sites that bind viral ssRNAs, whether this is specific over cellular RNAs and how VP6 interacts with genomic dsRNA, remain to be addressed.

In this study, we used RNA crosslinking and peptide fingerprinting (RCAP) to identify the RNA binding sites of VP6 using both a recombinant VP6 protein (reVP6) and in purified viral cores. The data demonstrate that multiple regions of reVP6 and core associated VP6 interact with both ssRNA and dsRNA but that each source of VP6 had a largely unique RNA binding profile with only one region in common. Mutagenesis of residues within the mapped RNA-binding regions followed by virus recovery using the RG system demonstrated that the VP6-RNA binding regions of the core associated VP6 were essential for BTV replication while those associated with reVP6 were dispensable. Within the essential binding sites, residues that recognize BTV RNA preferentially, possibly necessary for genome recruitment and packaging were identified. This study highlights the essential role of the orbivirus protein VP6 in genome packaging and replication.

MATERIAL AND METHODS

Virus, plasmids, mutagenesis and RNA transcripts synthesis

BTV-10 VP6 was used for the mutational analysis and reverse genetics (14, 16). BTV-1 (Genbank accession numbers FJ969719-FJ969728), which VP6 is fully exchangeable with BTV-10, was used in RCAP for viral capsids. All mutations of VP6 were generated by site-directed mutagenesis, sequences of these mutations and primers are available upon request. Transcripts for reverse genetic analyses were prepared using mMACHINE T7 transcription kit (Thermo); RNA transcripts for gel shifting and competition assay were prepared using T7 polymerase (Thermo), following manufacturers' instructions.

Recombinant VP6 (reVP6) expression and purification

The expression and purification of BTV-10 reVP6 using baculovirus in the Sf9 cell line was described previously (14). Additionally, His tagged wild-type (WT) and mutant reVP6 proteins were expressed in the *E. coli* strain BL21 (DE3) pLysS. The His-tagged reVP6 proteins were purified using Ni-NTA nickel affinity purification eluting the purified protein with buffer comprising 20 mM Tris-HCl, 200 mM NaCl, pH 7.4, and 250 mM imidazole. Imidazole was then removed by buffer exchange Sephadex G-75 columns (GE Healthcare).

RCAP

The RCAP assay was done as described previously (17, 18). For analysis of recombinant VP6 binding to RNA, one mole of RNA was added to two moles of recombinant protein. The molar ratio of RNA was kept low to decrease non-specific protein crosslinking to RNA. Formaldehyde was then added to a final concentration of 0.1% and incubated for 10 min at room temperature. Glycine was added to a concentration of 0.2 M for 10 min to quench additional crosslinking. The crosslinked protein-RNA complexes were digested using sequencing-grade trypsin (Trypsin Gold, Promega) for 16 h using a 1:20 (w/w) ratio of trypsin to capsid. RNA-peptide complexes were then selectively precipitated using a final concentration of 3 M lithium chloride and centrifugation at 16,000 x g. The peptide-RNA conjugates were reversed by a 1 h incubation at 70^{o}C. Parallel control reactions to assess background signals were performed without the addition formaldehyde or, in the case of the recombinant protein, without RNA. RCAP peptides were analysed using an Orbitrap Elite hybrid ion trap mass spectrometer equipped with an electrospray ionization source (ThermoFisher Scientific). The peptides were resolved using a Dionex UltiMate 3000 HPLC with a 1 x 150 mm Zorbax 300SB-C18 column (Agilent) and eluted using a linear gradient of 2–45% acetonitrile in water with 0.1% formic acid over 90 minutes with a flow rate of 50

µl/min. Tandem mass spectra were obtained using collision-induced dissociation in a data-dependent manner. Raw mass spectral data files were converted to mascot generic format and analysed using SearchGUI (19). Spectra were searched against a database of BTV proteins concatenated with the cRAP database (20). Unspecific enzyme cleavage and a mass tolerance of 10 ppm were used. Search results were compiled and visualized using PeptideShaker (21), and results were exported as a CSV file for automated processing with custom KNIME workflows (22).

Immunofluorescence staining and confocal microscopy

BSR cells transfected with 800 ng of VP6 capped S9 RNA containing wild type and mutant VP6 together with 800 ng of NS2 encoding capped S8 RNA by using Endofectin (GeneCopoeia), according to the manufacturer's instructions. 24 h post transfection cells were fixed with 4% paraformaldehyde (Sigma) solution, permeabilized with 0.5 % Triton X100 (Sigma), blocked with 1% BSA (Bovine Serum Albumin, Sigma), and subsequently stained using rabbit anti-NS2 and guinea pig anti-VP6 homemade primary antibodies, and anti-rabbit Alexa 546 and anti-guinea pig Alexa 488 coupled secondary antibodies (Thermo Fisher Scientific). Nuclei were stained using Hoechst 33342 (Thermo Fisher Scientific). Images were acquired using an x100 oil objective and a Zeiss Axiovert LSM510 confocal microscope supplied with the LSM510 software.

Circular dichroism (CD) spectra of reVP6

The CD spectra of reVP6 were recorded in CD buffer (20 mM Na_2HPO_4, 100mM NaCl, pH 7.4) at 20 °C. The far UV CD Spectral data were collected from 260–195 nm with a 0.5 mm rectangular cell path length at 20 °C on the Applied Photophysics Chirascan & Chirascan Plus spectrometers (Leatherhead, UK) attached to a Peltier unit (Quantum NorthWest TC125). The UV & CD spectra were smoothed (window factor of 4, Savitzky-Golay method) and analysed using Origin V6 and APL Prodata Viewer v4.2.15. The estimate of percentage secondary structural units (alpha helix and beta strand) of protein from the experimental CD spectra was calculated using K2D3 program as previously described (23).

Electrophoretic mobility shift assay (EMSA) using ^{32}P-labelled RNA

RNA labelling and the EMSA were performed as described previously (24). A typical binding assay of 20 µL contains 3 µg of reVP6 in the RNA binding buffer (2 mM $MgCl_2$, 60 mM KCl, 100 mM NaCl, 20 mM Hepes, pH 7.5, 10% glycerol, 1 unit of RNasin (Promega)). Radiolabelled BTV S10 was heated to 65°C for 2 min, the mixture of VP6 in binding buffer was added and incubated for 30 min at 4°C. Samples were then analysed on 0.8% agarose

gels in TBE (Tris borate-EDTA; 89 mM Tris, pH 7.4, 89 mM boric acid, 2.5 mM EDTA). The gels were dried and analysed by autoradiography or using Amersham Biosciences PhosphorImager. For competition assay, 18 nM of radiolabelled S10 RNA was incubated with 4 µM of reVP6 in presence of 1, 3, or 6 µg (85, 255, or 510 nM) of non-specific Xenopus elongation factor mRNA (Thermo Scientific). The mixture was analyzed as described.

Reverse genetics

Mutations in the cDNA of S9 RNA that encodes VP6 were generated using site-directed mutagenesis mutations (sequences available upon request), together with the other 9 BTV genome segments that were used to transfect BSR cells or a BSR cell line that stably expresses VP6 (BSR-VP6), as described by Boyce et al. (25). CPE was monitored after 3 days and the mutations in S9 in the recovered viruses was confirmed by RT-PCR and sequencing.

Plaque assay

WT and mutant viruses were diluted and applied to BSR cell monolayers at 0.01 to 0.1 MOI, covered by Avicel overlayers as described by Matrosovich et al. (26). Cells were fixed with formaldehyde and the plaque size monitored after 3 days.

Single cycle replication assay

WT BTV, VP6 truncated virus, and VP6 mutant viruses, were used to infect BSR cells or BSR cells that stably express VP6 (BSR-VP6). The cells were harvested at 12 hr post infection (hpi) and viral particles purified as described previously by Matsuo et al. (11). The purified virus was treated with RNaseA to remove non-packaged RNA. The RNA was extracted using a viral RNA purification kit (Thermo Fisher Scientifics). The positive and negative-sense RNA, representing genomic ssRNA and dsRNA respectively, were measured by qRT-PCR using viral RNA-specific primers (sequences available upon request) (27). To measure dsRNA synthesis, cell lysate at different time points were collected, immediately frozen in -80°C, and the quantity of ssRNA and dsRNA in the cell lysate were similarly measured with qRT-PCR.

***In vitro* cell-free assembly (CFA) assay**

The BTV *in vitro* assembly assay has been described previously (5). Briefly, the ten segments of ssRNA were incubated with VP1, VP4 and VP6, for 30 min, followed by adding VP3 and VP7 sequentially with a 1.5 hr incubation after each addition. As controls, the VP6 protein was either left out of the assembly reaction, or added after VP3. To avoid the VP6

protein being translated from the S9 of the ten ssRNAs, we used a vaccine strain S9 RNA, which does not translate VP6. The samples were then subjected to a 15%-65% sucrose gradient and the packaged RNA quantified with qRT-PCR.

RNA binding assay

5 µg of purified WT or mutant His-tag VP6 were bound with 30 µl of Ni-NTA agarose beads (Thermo) in a buffer of 150 mM NaCl and 40 mM Tris-HCl pH 8.0. The protein-coated beads were then incubated with 0.3 µg (1.1 pmol) of BTV S10 RNA in the presence or absence of 30 µg (1 nmol) of yeast tRNA. After extensive washes, the bound RNA was eluted by heating and quantified by qRT-PCR.

qRT-PCR

The extracted viral RNA from the single cycle replication and CFA assay was subjected to RT reaction, using specific BTV S6 forward or reverse primers, followed by qPCR, using SYBR-Green master mix (Labtech) and S6 primers (27). RNA eluted from VP6-RNA beads binding assay was quantified using specific BTV S10 primers.

238 **RESULTS**

239 **Genomic ssRNA is not packaged in the viral capsid in the absence of VP6**

240 During BTV replication, newly synthesised ssRNA segments are first packaged into the
241 assembling viral cores, which in turn serve as templates for the synthesis of genomic dsRNA
242 segments (5). VP6 has been shown to be an essential component of the primary replication
243 complex and has been hypothesized to function in recruiting and packaging BTV RNA (9,
244 10, 13). Rescued BTV carrying a truncated VP6 was only possible in a VP6 complementary
245 cell line and although these rescued VP6-defective viruses could express BTV proteins on
246 infection, they assembled only a low level of particles, which lacked the viral genome as
247 visualized by electron microscopy (11). To confirm correlation between a functional VP6 and
248 RNA packaging, an available BTV strain with a truncated VP6 (triple stop codons introduced
249 at residues 87-89 (28)) was grown in a VP6-complementing BSR-derived cell line (BSR-
250 VP6) and, after 3 days, the recovered virion particles were used to infect both parental BSR
251 cells and BSR-VP6 cells. Although these particles lacked the S9 RNA segment that encodes
252 VP6, they still contained VP6 protein incorporated from BSR-VP6 cells used to recover the
253 virus and thus were capable of synthesizing first round ssRNAs, although not capable of
254 completion of replication or second round transcription following infection of WT BSR cells.
255 Newly synthesised viral particles were harvested after 12 hours, the result of only one
256 replication cycle. The packaged RNA was quantified by qRT-PCR, assaying for both positive
257 and negative strands of S6 RNA with a S6 RNA segment-specific probe. While both the
258 positive and negative strands of RNA molecules were present in the particles recovered from
259 BSR-VP6 cells, particles from normal cells had less than 3% of the amount observed in the
260 BSR-VP6 cells grown particles (Figure 1A). This low-level signal is most likely residual RNA
261 from the inoculum. These data confirm that in the absence of functional VP6 newly
262 synthesized viral RNA segments are not packaged, consistent with a role in the packaging of
263 viral RNA. As a control, we measured the BTV ssRNA in the cell lysate from BSR-VP6 or
264 BSR cells infected with VP6-truncated particles (Figure 1B). BTV ssRNA transcripts were
265 synthesized abundantly in both cell lines, slightly more so in BSR-VP6 cells than the WT
266 BSR cells.
267
268 To investigate at which stage VP6 can affect virus assembly, we used the established *in*
269 *vitro* cell-free assembly (CFA) assay (5). In this assay, the ten ssRNA segments of BTV are
270 first incubated with replicase complex proteins VP1, VP4 and VP6, followed by the
271 incubation with the inner capsid proteins VP3 and VP7, to assemble a core particle. We
272 modified this assay for our study by either excluding VP6, or by including it after the addition
273 of VP3, so that it should not be incorporated into the core particle. The amount of RNA
274 encapsidated was then quantified using RT-PCR as before. In the absence of VP6, ssRNA

packaging was reduced to less than 10% of the control (Figure 1C). Further, the addition of VP6 after VP3, which forms the inner layer of the core, failed to rescue RNA packaging. These data further suggest that VP6 plays a role in the early stage of genomic ssRNA packaging prior to inner core assembly.

Identification of the RNA binding sites of VP6 and their impact on virus replication

VP6 has a high number of charged residues and readily binds non-specific ssRNA and dsRNA *in vitro* (16, 29). We sought to identify the RNA binding regions in VP6 using a proteomic-based RCAP method. For the RCAP analysis, we used S10, the smallest of the BTV RNA segments and a recombinant VP6 (reVP6) expressed in the baculovirus expression system. Two independent experiments, each with independent samples replicated in triplicate, identified very similar RNA binding regions within reVP6 (Figure 2), indicating that such an approach can reproducibly identify residues that contact RNA. All of the peptides were not present in reactions lacking RNA and the majority are also absent in control reactions that were not crosslinked with formaldehyde (Table 1). Three regions of VP6 were strongly associated with binding ssRNA: aa2-15 (Re1), aa110-141 (Re2) and aa220-284 (Re3) (Figure 2). To assess whether these *in vitro* RNA-binding sites are important for virus replication, six positively-charged sites within VP6 (KR_{14-5}, K_{110}, K_{131}, K_{141}, KK_{246-7}, RK_{257-8}) were selected for substitution mutagenesis. To perturb the potential RNA binding affinity, each residue was substituted for glutamic acid (Glu, E), either individually (K_{110}, R_{131}, R_{141}) or as double substitution mutations (KR_{14-5}, KK_{246-7}, RK_{257-8}). Each of these mutant segments, together with the other nine WT BTV RNA segments, were then transfected into BSR cells for virus recovery.

Mutations in Re1 (KR_{14-5}EE) or Re2 (K_{110}E, R_{131}E, and R_{141}E) did not affect virus recovery; recovered mutant viruses produced plaques with a similar size to the parental virus (Figure 3A). DNA sequencing confirmed the presence of the mutations within S9 for all recovered viruses and the absence of compensatory mutations elsewhere. In contrast, the double mutations located within the RNA binding region Re3 (KK_{246-7}EE and RK_{257-8}EE) prevented virus recovery despite several independent attempts. To examine this further, two pairs of negatively-charged residues from a conserved Glu rich motif (EE-K-XX-EE) in the same Re3 region were also mutated to neutral charged glutamine (EE_{225-6}QQ and EE_{230-1}QQ). Both mutant constructs were then tested for their impact on virus recovery by RG. In both cases, the virus was successfully recovered, suggesting that positively-charged residues in region Re3, but not the negatively-charged residues, are important for viral infection. The positively-charged residues located in RNA binding region Re3 are thus essential for virus replication.

Although VP6 binds both ssRNA and dsRNA (16) it is not known if the sites concerned are the same. To investigate this, BTV genomic dsRNA segments were isolated from BTV infected cells and the RCAP analysis with reVP6 was repeated using dsRNA. The dsRNA-binding regions identified were similar with those that bind ssRNA (Figure 2, Table 1), suggesting that, in the absence of other viral proteins, VP6 binds ssRNA and dsRNA in a similar manner.

Identification of VP6-RNA binding regions within the viral capsid and their importance on virus replication

Recombinant VP6 has multiple regions that contacts ssRNA and dsRNA. However, VP6 found in the virus cores are in contact with capsid protein and this could impact RNA binding. To examine this, we purified mature cores and subjected them to RCAP analysis (Figure 2). Peptides from several core-associated proteins were identified and those from VP6 were assigned based on collision-induced fragmentation of each peptide. Within VP6, four regions were found to contact the encapsidated genomic dsRNA: residues aa151-177 (Ca1), aa246-257 (Ca2), aa281-300 (Ca3) and aa305-328 (Ca4). Notably, only Ca2 overlaps with the RNA-binding region 3 found when the analysis was done with reVP6. Thus, core-associated VP6 has a different binding profile to recombinant VP6. To map the essential binding sites a number of positively-charged residues in the identified Ca regions were targeted for site-directed mutagenesis and virus recovery using RG system. Five site-specific mutations were introduced, $R_{167}E$ and $R_{177}E$, located in region Ca1, $K_{296}E$ in region Ca3, $KRR_{303\text{-}5}EEE$ and $K_{318}E$ in region Ca4. Among the five mutations introduced into VP6, only $K_{318}E$, permitted recovery of viruses with normal plaque size (Figure 3B). All other mutations abrogated virus recovery. Consistent with previous data, the two positively-charged sites ($KK_{246\text{-}7}EE$ and $RK_{257\text{-}8}EE$) in the Ca2/Re3 shared region (Ca2/Re3) were lethal confirming these regions as critical for virus replication. Residues $RK_{208\text{-}209}$ of VP6 that were previously proposed to contact BTV RNA by bioinformatics analysis, were not identified by RCAP (14). In contrast to the Ca mutants, a $RK_{208\text{-}209}EE$ VP6 mutant did not perturb virus recovery, demonstrating that RCAP is more precise method for recognizing RNA-contacting residues.

Previous data has suggested that certain RNA sequences in the BTV genome, especially in the smaller RNA segments, act as packaging signals that mediate RNA assembly through RNA-RNA interaction (1, 15). To ensure that the mutations introduced into the S9 RNA sequence encoding VP6 did not affect RNA packaging, the lethal mutations described above were also rescued using a RG system in the VP6-complementary BSR-VP6 cells (9). Viruses with mutations in all six Ca regions produced the virus in BSR-VP6 cells.

Furthermore, the rescued virus failed to grow when passaged on normal BSR cells. These results confirmed that the lethal effect of these mutations was due to changes in VP6 protein, not due to a change in the packaging signals in S9 RNA.

To exclude the concern that substitutions of negatively-charged residues influences protein conformation or isoelectric point, five lethal mutations were also redesigned to change the positively-charged R or K into alanine (Ala, A) ($R_{167}A$, $R_{177}A$, $KK_{246-7}AA$, $RK_{257-8}AA$, and $K_{296}A$). None of these mutants was recovered following RG transfection in the normal BSR cells (data not shown). However, when S9 RNA carrying critical Ca2/Re3 region mutations ($KK_{246-7}EE$, $RK_{257-8}EE$, $KK_{246-7}AA$ and $RK_{257-8}AA$) were transfected into BSR cells, all the mutant VP6 expressed in the cells and the localization was not different from WT VP6 (Figure 4).

To ensure no gross conformational change in the mutation mapped as critical, several mutant VP6 proteins were expressed in *E. coli*, purified and analysed by gel electrophoresis and for secondary structure. Each mutant VP6 exhibited the same mobility as the WT VP6 (Figure 5A) and when analysed by circular dichroism (CD) spectroscopy, all showed similar spectra except a slight difference with $RK_{208-9}EE$ and $KRR_{303-5}EEE$ compared to the WT. However, relative values of alpha helix and beta sheet did not vary beyond the variance of the assay (Figure 5B and Table 2). We calculated the secondary structure elements using tool K2D3. The change in % of individual secondary structure components clearly showed it is not significant.

Taken together, these data suggest that mutations introduced into VP6 to probe its RNA binding function studied here did not induce major conformational change in any of the mutants described.

The lethal VP6 mutant lacks preferential binding affinity for viral RNA

BTV S10 ssRNA was previously found to be critical for efficient RNA packaging (1, 15, 30) and was therefore used as the source of RNA to investigate the preference of the RNA binding by VP6. VP6 binding to S10 RNA was examined using ^{32}P-labelled S10 RNA by a gel electrophoretic mobility shift assay (EMSA). Three recombinant VP6 proteins were tested, a replication competent mutant, $RK_{208-9}EE$, a replication incompetent mutant, $RK_{257-8}EE$, which is located within the Ca2/Re3 region and WT reVP6. In the EMSA, all three proteins exhibited strong band retardation, plausibly a measure of the non-specific RNA binding function described above (Figure 6A). To investigate preferential binding by VP6 an alternate, competition method of RNA-protein interaction was used. S10 ssRNA was

386 exposed to Ni-NTA agarose beads coated with His-tagged WT reVP6 or $RK_{257-8}EE$ mutant in
387 the presence or absence of an excess of yeast tRNA and, after pull-down, the bound RNA
388 was quantified by qRT-PCR. The amount of RNA bound was not significantly affected in the
389 presence of excess yeast tRNA for WT reVP6 while for the $RK_{257-8}EE$ mutant the presence
390 of excess tRNA significantly reduced the level of S10 RNA bound (Figure 6B).
391
392 To confirm this in a quantitative manner, we performed competition assay in presence of
393 different quantities of non-specific RNA (Figure 7). To exclude the possibility that the
394 difference in binding was due to small size of the competitor tRNA, we used a longer ssRNA
395 encoding Xenopus elongation factor 1α as a non-specific RNA. Further, to ensure the RNA
396 binding was not influenced by changes in charge, we expressed the mutant $RK_{257-8}AA$ in *E*
397 *coli*, purified and utilized for EMSA. The data showed that $RK_{257-8}AA$ reVP6 had much lower
398 preferential binding with BTV RNA compared to WT reVP6 (Figure 7B). Moreover, when an
399 additional positively-charged site RK_{246-7} within the same Ca2/Re3 region, was mutated to
400 Ala, it also exhibited a significant effect on the preference of VP6 for BTV RNA (Figure 7C).
401 However, the replication competent mutant, $RK_{208-9}EE$, exhibited gel shifting patterns similar
402 to the WT reVP6 (Figure 7D). These results indicate that the Re3/Ca2 region in VP6 is part
403 of a preferential BTV RNA binding site.
404
405 **Mutant VP6 is unable to package viral RNAs**
406 The Ca2/Re3 region binds both ssRNA *in vitro* and dsRNA in the viral capsid. Further, it
407 exhibits preference for BTV RNA, consistent with a key role in the recruitment of ssRNA into
408 assembling capsids. To confirm this, we employed the *in vitro* CFA assay, which had already
409 demonstrated that RNA packaging was dependent on VP6. Making use of the $RK_{257-8}EE$
410 VP6 mutant, WT VP6 (positive control) or no VP6 (negative control) the level of incorporated
411 genomic RNAs in the *in vitro* assembled cores was measured by qRT-PCR. RNA packaging
412 was significantly reduced compared to WT when the RK_{257-8} mutant protein was present,
413 almost to the background level of incorporation observed in the absence of VP6 (Figure 8).
414 To assess if a similar effect occurs in infected cells, $RK_{257-8}EE$ mutant virus grown in the
415 BSR-VP6 helper cell line was used to infect the parental BSR cell line for 6 hrs and total
416 RNA was extracted from 0 to 6 hpi. As control, BSR-VP6 cells, which are permissive for the
417 growth of the mutant, were also infected with the same virus preparation and RNA extracted.
418 All RNA samples were analysed by qRT-PCR using primers specific for the detection of
419 positive or negative-sense RNA, as previously described. In this analysis quantification of
420 the negative strand act as a marker for dsRNA synthesis as previously described (5, 11).
421 During the infected period, a similar quantity of positive-sense BTV-RNA was produced by
422 the mutant virus in both cell lines. However, in the parental BSR cells negative-sense RNA

synthesis was reduced to ~1000 folds at 6 hpi, when compared to the parental virus (Figure 9). These data are consistent with VP6 acting in the packaging of BTV RNA into the core via preferential recognition by the Ca2/Re3 region.

DISCUSSION

Previous reports have implicated VP6, a protein with clusters of charged residues, in the packaging of the viral genomic RNA, but precise mapping of the binding sites and their contribution to virus replication was not reported (8, 11, 13, 14, 16). We used a robust peptide mapping method, RCAP, which could identify interactions between VP6 and the viral genome in the natural state leading to the identification of four (Ca) VP6-BTV RNA binding sites. When compared to binding sites mapped by the binding of recombinant (Re) VP6 to RNA *in vitro*, several regions were distinct suggesting that the RNA binding by VP6 contains both specific and non-specific elements. Mutations in the Ca RNA binding sites targeting positively-charged residues (R_{167}, R_{177}, KK_{246-7}, RK_{257-8}, K_{296}, and KRR_{303-5}) prevented virus recovery irrespective of the charge status of the mutated residues. These six sites are highly conserved among the VP6 of different BTV serotypes and the related orbiviruses EHDV and AHSV. This suggests the interaction between VP6 and RNA within the core is invariant consistent with a key functional role.

More recently, a specific site of VP6 (aa276-287) was reported to interact with the inner layer capsid protein VP3, an interaction that was essential for virus assembly (8). This interaction site is distinct from the RNA interaction sites reported here suggesting it may act to bridge the captured genomic RNA with the assembling capsid. Some viruses, such as bacteriophage MS2 use their coat protein to package genomic RNA through specific signals (31, 32) but for complex, multi-layered capsid viruses, such as orbiviruses, genome packaging is likely to engage more than one viral protein. The two different kinds of interactions that are seen in BTV, VP6-VP3 and VP6-RNA, are consistent with this hypothesis.

In contrast, RCAP analysis of the *in vitro* RNA-binding regions of reVP6, were largely not specific, a conclusion supported by the EMSA data. The amino terminal region (Re1) of reVP6 is also conserved among the Orbiviruses but changing the only positively-charged residues in this region, KR_{14-5}, did not influence virus replication suggesting this conservation of amino acid sequence is due to other functional reasons. The disorder prediction of VP6 structure showed that the N-terminal part of VP6 was more disordered than the C-terminal part, suggesting the N-terminus is highly mobile with non-specifc binding while the C-terminus with a conserved function, which was consistent with our findings (33). Previous study suggested that only hexameric form of VP6 could perform helicase activity *in vitro*, although monomeric VP6 could still bind RNA (14, 16). However, it is still not known what form of VP6 exists within the viral capsid and in cells when it functions as an RNA binding

protein. The relationship between VP6 oligomerization and its different functions required further investigation.

One region revealed by the comparative RCAP analysis (aa246-257; amino acid sequence: KKLLSMIGGVERK) was associated with RNA binding both *in vitro* and in the viral capsid. This region has two sites, each with two positively-charged residues, KK_{246-7} and RK_{257-8} and both were shown to be essential for viral replication. The same mutations led to VP6 losing its preference for BTV RNA in completion binding assays suggesting the region is part of discriminatory mechanism which selects BTV RNA over the cellular pool. This observation of preferential binding could be due to the region of VP6 recognizing certain sequences or secondary structures in the viral RNA segments. However, the precise sequence(s) that VP6 binds during packaging and if VP6 plays an active role in the RNA complex formation remain to be investigated.

In an earlier report, a cell-free assembly assay was established whereby the sequential mixing of replicase proteins VP1, VP4, and VP6, together with BTV ssRNAs, followed by the sequential addition of the inner capsid proteins VP3 and VP7, resulted in the successful packaging of ssRNAs into a core structure (5). In the absence of VP6 during sequential assembly packaging of ssRNAs is not observed, again consistent with a role for VP6 in the packaging of ssRNA into the BTV core structure. When a single cycle infection assay was performed with the RK_{257-8} mutant virus, amplified in a helper cell line, despite still being able to synthesize positive-sense viral ssRNAs, only low levels of negative-sense RNAs were detected, insufficient to support viral rescue. These data may indicate a marginal VP6 activity, below the threshold required for growth or the residual activity of the VP6 incorporated form the BSR-VP6 cell used for mutant virus recovery. These data clearly indicate that VP6 is critical in an early function, such as selectively binding to BTV RNA, and that the region encompassing aa246-257 is a required motif.

Viral protein helps RNA virus to package correctly its genome through diverted mechanism. Besides the bacteriophage coat protein mentioned above, dsRNA bacteriophages of the Cystoviridae family contains a hexametic ATPase, P4, serves as RNA packaging motor (34, 35). Recently, alphatetravirus was found to have a small encapsidated protein P17 that specifically binds to viral RNA and assist RNA packaging (36). Orbivirus VP6, despite some similarities with other packaging proteins, appears to have its unique mechanism.

Previous study have suggested ATPase motif and helicase motif of VP6 based on *in vitro* functional analysis (14). K_{110}, the previously reported ATPase motif, was in the RCAP

identified RNA binding region (Re2). However, changing this site also did not influence virus replication. E_{157}, a site in the previously suggested helicase (DEAD box) also did not show any influence on virus grow (unpublished observation). Both these two sites are conserved within BTV but not shared with EHDV or AHSV. Studies have shown that ATP-driven duplex unwinding function is not necessarily the primary mechanism of helicase proteins (37, 38). Helicase protein can serve as translocator without unwinding the duplex (39-42). Further investigation is required to clarify the role of ATPase and helicase activity of VP6 during genome packaging.

It is highly likely that RNA segments interact with each other in a sequential manner prior to the RNA complex packaging into capsid (1, 5, 15). In our recent report we showed that the RNA segments assortment is mainly based on RNA-RNA interactions via specific sequences (43). It is possible that VP6 may also be actively involved in assortment, but our current data does not support this notion.

Structural analysis showed that VP1 and VP4 could be encapsidated within the core-like particles of VP3 and VP7, whilst VP6 alone could not be encapsidated without viral RNA (7). It can be hypothesized that not only is VP6 essential for genome packaging, but also, perhaps reciprocally, that genomic RNA plays a role in VP6 encapsidation. More detailed structural and functional studies are required to elucidate further the protein-RNA arrangements in the viral capsid, and precisely how these interactions promote genome packaging during capsid assembly.

ACKNOWLEDGEMENT

We thank C.C. Celma for providing BTV core sample, T. Fajardo for helping in the RG experiment and D. Villani for helping the mutant constructs cloning. We also thank Tam Bui of the Bimolecular Spectroscopy Centre, King's College London who helped with collection of CD data.

FUNDING

This work was supported by the US National Institutes of Health (R01AI045000), and partly by the UK Biotechnology and Biological Sciences Research Council (BB/P00542X) and Wellcome Trust, UK (100218, Investigator Award to PR). Funding for open access charge: National Institutes of Health (R01AI045000).

CONFLICT OF INTEREST

The authors declare no conflict of interest.

539

FIGURE LEGENDS

Figure 1. RNA packaging in viral particles relied on VP6. (A) VP6 truncated virus was used to infect BSR or BSR-VP6 cells, 12 hours later the viral particles were harvested and purified, and the positive (+) and negative (-) strand, representing genomic ssRNA and dsRNA respectively, were measured by qRT-PCR. (B) BTV ssRNAs in the cell lysate from (A) were measured by qRT-PCR (C) CFA assay was performed in original method (control), in absence of VP6 (no VP6), or adding VP6 at later time point (late VP6 adding). The assembled complex was purified and packaged and viral RNA measured by qRT-PCR. The mean values ±SD are shown (n=3).

Figure 2. **Regions of the BTV VP6 that contacts RNA.** The grey bar represents the VP6 protein, with the vertical dashes denoting the positions of positively and negatively-charged amino acids. The thick black lines represent peptides identified in the RCAP analyses performed with recombinant VP6 protein (reVP6) and either single-stranded or double-stranded RNAs and from purified cores. Details of the peptides are presented in Table 1. The three regions in reVP6 contact RNAs are named Re1-3. Regions in the core-associated VP6 that contact packaged genomic RNAs are named Ca1-4. Mutations were introduced on 13 specific charged sites (number 1-13) and the sites that mutations had lethal effect indicated (*).

Figure 3. Plaque formations of WT and mutant viruses.

Figure 4. Mutant VP6 express similar to WT VP6. Four mutants ($RK_{246-7}AA$, $RK_{246-7}EE$, $RK_{257-8}AA$ and $RK_{257-8}EE$) and wild type (WT) VP6 encoding S9 RNAs were used to transfect BSR cells. Protein expression and localization were monitored by immunofluorescence staining and confocal microscopy. Green: VP6; blue: Hoechst staining.

Figure 5. Conformational analysis of mutant reVP6. (A) Five mutant reVP6 protein were expressed in *E. coli* and analyzed by SDS-PAGE together with wild type (WT) VP6, followed by coomassie blue staining. The sizes of protein ladder (M) are indicated. (B) The figure shows CD spectra of VP6 mutants normalized to wild type VP6. Each mutant and wild-type VP6 are indicated with different colours.

Figure 6. VP6 shows BTV RNA binding preference. (A) Two mutant VP6 protein, $RK_{208-9}EE$ and $RK_{257-8}EE$, together with WT VP6, were incubated with ^{32}P-labelled BTV S10

ssRNA for interaction. The shifting of the VP6-RNA complex was subjected to EMSA using 0.8% agarose gel and TBE buffer before being analysed with phosphorimager. (B) WT or $RK_{257-8}EE$ reVP6 were bound to Ni-beads and incubated with BTV ssRNA S10, in absence or presence of 100 folds quantity of tRNA (+tRNA). The bound RNA was then eluted and quantified with qRT-PCR. The mean values ±SD are shown (n=3).

Figure 7. Mutations in Ca2/Re3 region destroys BTV RNA preferential binding. Competition assay was performed using 1µg of WT (A), $RK_{257-8}AA$ (B), $KK_{246-7}AA$ (C), or $RK_{208-9}EE$ reVP6 (D) and 0.1µg of ^{32}P-labelled BTV S10. Xenopus elongation factor (Xef) mRNA was added in quantities as indicated. The free S10 RNA size is indicated.

Figure 8. Mutation on VP6 prohibits genomic RNA packaging. CFA assay was performed in the presence of WT VP6 (control), $RK_{257-8}EE$ VP6, or in absence of VP6 (no VP6). The assembled complex was purified and the packaged viral RNA measured by qRT-PCR. The mean values ±SD are shown (n=3).

Figure 9. VP6 mutant virus is deficient in producing dsRNA genome. The VP6 $RK_{257-8}EE$ mutant virus was used to infect BSR cells ($RK_{257-8}EE$, red line) or BSR-VP6 cells (WT, blue line). Total cytoplasmic RNA was harvested at 0, 2, 4, and 6 hpi. The positive (+) and negative (-) strand RNA representing genomic ssRNA (left panel) and dsRNA (right panel) respectively, were measured by qRT-PCR. The mean values ±SD are shown (n=3).

REFERENCES

1. Fajardo T, Jr., Sung PY, Roy P. 2015. Disruption of Specific RNA-RNA Interactions in a Double-Stranded RNA Virus Inhibits Genome Packaging and Virus Infectivity. PLoS Pathog 11:e1005321.
2. Patel A, Roy P. 2014. The molecular biology of Bluetongue virus replication. Virus Res 182:5-20.
3. Roy P. 2008. Bluetongue virus: dissection of the polymerase complex. J Gen Virol 89:1789-804.
4. Roy P. 2017. Bluetongue virus structure and assembly. Curr Opin Virol 24:115-123.
5. Lourenco S, Roy P. 2011. In vitro reconstitution of Bluetongue virus infectious cores. Proc Natl Acad Sci U S A 108:13746-51.
6. Diprose JM, Burroughs JN, Sutton GC, Goldsmith A, Gouet P, Malby R, Overton I, Zientara S, Mertens PP, Stuart DI, Grimes JM. 2001. Translocation portals for the substrates and products of a viral transcription complex: the bluetongue virus core. EMBO J 20:7229-39.
7. Nason EL, Rothagel R, Mukherjee SK, Kar AK, Forzan M, Prasad BV, Roy P. 2004. Interactions between the inner and outer capsids of bluetongue virus. J Virol 78:8059-67.
8. Matsuo E, Yamazaki K, Tsuruta H, Roy P. 2018. Interaction between a Unique Minor Protein and a Major Capsid Protein of Bluetongue Virus Controls Virus Infectivity. J Virol 92.
9. Matsuo E, Roy P. 2009. Bluetongue virus VP6 acts early in the replication cycle and can form the basis of chimeric virus formation. J Virol 83:8842-8.
10. Matsuo E, Celma CC, Boyce M, Viarouge C, Sailleau C, Dubois E, Breard E, Thiery R, Zientara S, Roy P. 2011. Generation of replication-defective virus-based vaccines that confer full protection in sheep against virulent bluetongue virus challenge. J Virol 85:10213-21.
11. Matsuo E, Roy P. 2013. Minimum requirements for bluetongue virus primary replication in vivo. J Virol 87:882-9.
12. Kar AK, Bhattacharya B, Roy P. 2007. Bluetongue virus RNA binding protein NS2 is a modulator of viral replication and assembly. BMC Mol Biol 8:4.
13. Stauber N, Martinez-Costas J, Sutton G, Monastyrskaya K, Roy P. 1997. Bluetongue virus VP6 protein binds ATP and exhibits an RNA-dependent ATPase function and a helicase activity that catalyze the unwinding of double-stranded RNA substrates. J Virol 71:7220-6.
14. Kar AK, Roy P. 2003. Defining the structure-function relationships of bluetongue virus helicase protein VP6. J Virol 77:11347-56.
15. Sung PY, Roy P. 2014. Sequential packaging of RNA genomic segments during the assembly of Bluetongue virus. Nucleic Acids Res 42:13824-38.
16. Roy P, Adachi A, Urakawa T, Booth TF, Thomas CP. 1990. Identification of bluetongue virus VP6 protein as a nucleic acid-binding protein and the localization of VP6 in virus-infected vertebrate cells. J Virol 64:1-8.
17. Shakeel S, Evans JD, Hazelbaker M, Kao CC, Vaughan RC, Butcher SJ. 2018. Intrinsically-disordered N-termini in human parechovirus 1 capsid proteins bind encapsidated RNA. Sci Rep 8:5820.
18. Vaughan RC, Kao CC. 2015. Mapping protein-RNA interactions by RCAP, RNA-cross-linking and peptide fingerprinting. Methods Mol Biol 1297:225-36.
19. Wang X, Jones DR, Shaw TI, Cho JH, Wang Y, Tan H, Xie B, Zhou S, Li Y, Peng J. 2018. Target-Decoy-Based False Discovery Rate Estimation for Large-Scale Metabolite Identification. J Proteome Res 17:2328-2334.
20. Mellacheruvu D, Wright Z, Couzens AL, Lambert JP, St-Denis NA, Li T, Miteva YV, Hauri S, Sardiu ME, Low TY, Halim VA, Bagshaw RD, Hubner NC, Al-Hakim A, Bouchard A, Faubert D, Fermin D, Dunham WH, Goudreault M, Lin ZY, Badillo BG, Pawson T, Durocher D, Coulombe B, Aebersold R, Superti-Furga G, Colinge J, Heck

AJ, Choi H, Gstaiger M, Mohammed S, Cristea IM, Bennett KL, Washburn MP, Raught B, Ewing RM, Gingras AC, Nesvizhskii AI. 2013. The CRAPome: a contaminant repository for affinity purification-mass spectrometry data. Nat Methods 10:730-6.

21. Vaudel M, Burkhart JM, Zahedi RP, Oveland E, Berven FS, Sickmann A, Martens L, Barsnes H. 2015. PeptideShaker enables reanalysis of MS-derived proteomics data sets. Nat Biotechnol 33:22-4.

22. Berthold MR. 2008. KNIME: The Konstanz Information Miner, p 319-326. *In* Preisach C. BH, Schmidt-Thieme L., Decker R. (ed), Data Analysis, Machine Learning and Applications doi:https://doi.org/10.1007/978-3-540-78246-9_38. Springer, Berlin, Heidelberg.

23. Louis-Jeune C, Andrade-Navarro MA, Perez-Iratxeta C. 2012. Prediction of protein secondary structure from circular dichroism using theoretically derived spectra. Proteins 80:374-81.

24. Lymperopoulos K, Wirblich C, Brierley I, Roy P. 2003. Sequence specificity in the interaction of Bluetongue virus non-structural protein 2 (NS2) with viral RNA. J Biol Chem 278:31722-30.

25. Boyce M, Celma CC, Roy P. 2008. Development of reverse genetics systems for bluetongue virus: recovery of infectious virus from synthetic RNA transcripts. J Virol 82:8339-48.

26. Matrosovich M, Matrosovich T, Garten W, Klenk HD. 2006. New low-viscosity overlay medium for viral plaque assays. Virol J 3:63.

27. Toussaint JF, Sailleau C, Breard E, Zientara S, De Clercq K. 2007. Bluetongue virus detection by two real-time RT-qPCRs targeting two different genomic segments. J Virol Methods 140:115-23.

28. Celma CC, Stewart M, Wernike K, Eschbaumer M, Gonzalez-Molleda L, Breard E, Schulz C, Hoffmann B, Haegeman A, De Clercq K, Zientara S, van Rijn PA, Beer M, Roy P. 2017. Replication-Deficient Particles: New Insights into the Next Generation of Bluetongue Virus Vaccines. J Virol 91.

29. Fukusho A, Yu Y, Yamaguchi S, Roy P. 1989. Completion of the sequence of bluetongue virus serotype 10 by the characterization of a structural protein, VP6, and a non-structural protein, NS2. J Gen Virol 70 (Pt 7):1677-89.

30. Boyce M, McCrae MA. 2015. Rapid mapping of functional cis-acting RNA elements by recovery of virus from a degenerate RNA population: application to genome segment 10 of bluetongue virus. J Gen Virol 96:3072-82.

31. Dykeman EC, Stockley PG, Twarock R. 2013. Packaging signals in two single-stranded RNA viruses imply a conserved assembly mechanism and geometry of the packaged genome. J Mol Biol 425:3235-49.

32. Rolfsson O, Middleton S, Manfield IW, White SJ, Fan B, Vaughan R, Ranson NA, Dykeman E, Twarock R, Ford J, Kao CC, Stockley PG. 2016. Direct Evidence for Packaging Signal-Mediated Assembly of Bacteriophage MS2. J Mol Biol 428:431-48.

33. Matsuo E, Leon E, Matthews SJ, Roy P. 2014. Structure based modification of Bluetongue virus helicase protein VP6 to produce a viable VP6-truncated BTV. Biochem Biophys Res Commun 451:603-8.

34. Mancini EJ, Kainov DE, Grimes JM, Tuma R, Bamford DH, Stuart DI. 2004. Atomic snapshots of an RNA packaging motor reveal conformational changes linking ATP hydrolysis to RNA translocation. Cell 118:743-55.

35. Mancini EJ, Tuma R. 2012. Mechanism of RNA packaging motor. Adv Exp Med Biol 726:609-29.

36. Mendes A, Vlok M, Short JR, Matsui T, Dorrington RA. 2015. An encapsidated viral protein and its role in RNA packaging by a non-enveloped animal RNA virus. Virology 476:323-333.

37. Jankowsky E, Fairman ME. 2007. RNA helicases--one fold for many functions. Curr Opin Struct Biol 17:316-24.

38. Mayas RM, Staley JP. 2006. DEAD on. Nat Struct Mol Biol 13:954-5.

39. Soultanas P, Dillingham MS, Wiley P, Webb MR, Wigley DB. 2000. Uncoupling DNA translocation and helicase activity in PcrA: direct evidence for an active mechanism. EMBO J 19:3799-810.
40. Seidel R, Bloom JG, Dekker C, Szczelkun MD. 2008. Motor step size and ATP coupling efficiency of the dsDNA translocase EcoR124I. EMBO J 27:1388-98.
41. Myong S, Cui S, Cornish PV, Kirchhofer A, Gack MU, Jung JU, Hopfner KP, Ha T. 2009. Cytosolic viral sensor RIG-I is a 5'-triphosphate-dependent translocase on double-stranded RNA. Science 323:1070-4.
42. Durr H, Flaus A, Owen-Hughes T, Hopfner KP. 2006. Snf2 family ATPases and DExx box helicases: differences and unifying concepts from high-resolution crystal structures. Nucleic Acids Res 34:4160-7.
43. AlShaikhahmed K, Leonov G, Sung PY, Bingham RJ, Twarock R, Roy P. 2018. Dynamic network approach for the modelling of genomic sub-complexes in multi-segmented viruses. Nucleic Acids Res doi:10.1093/nar/gky881.

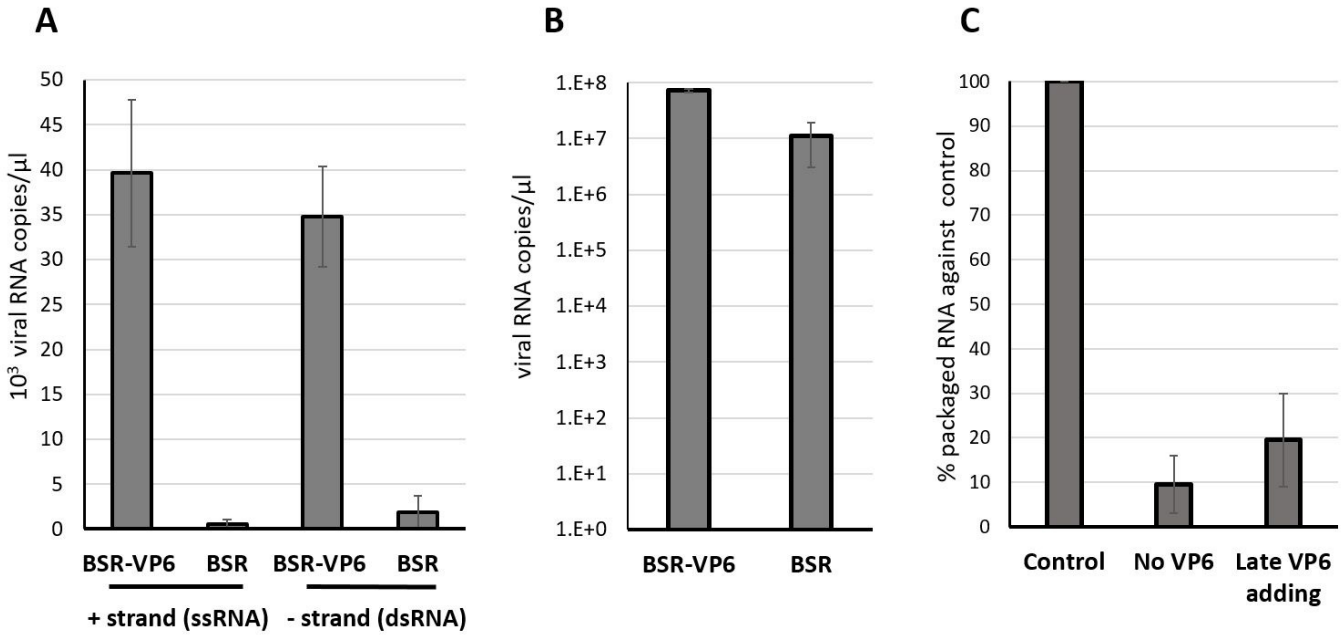

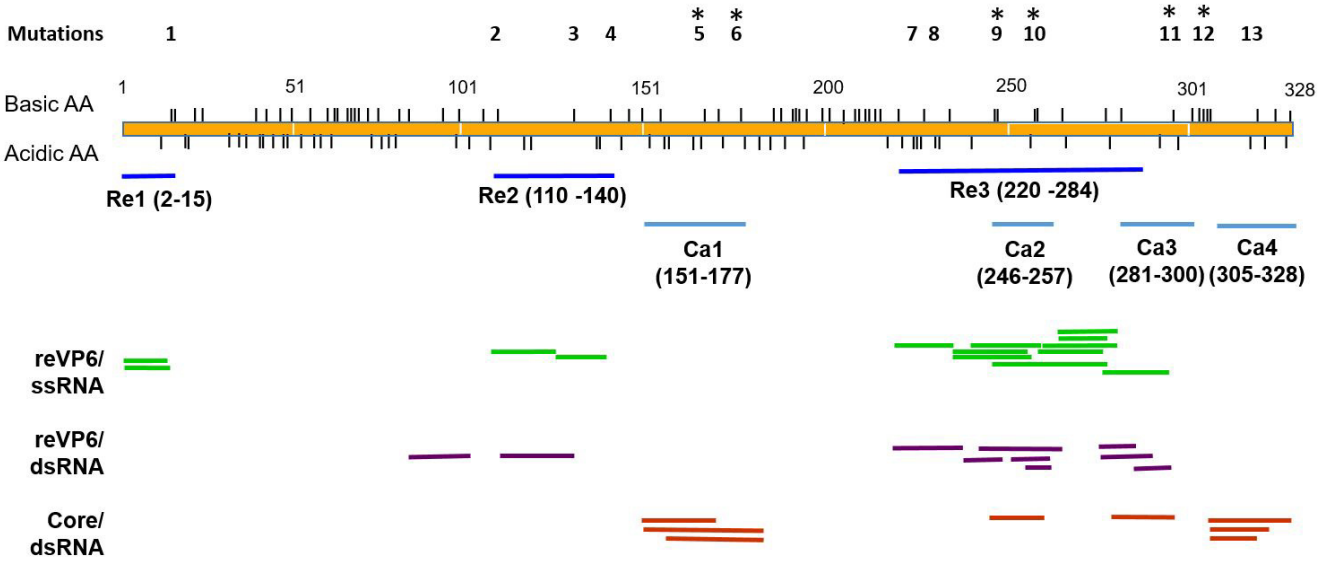

Journal of Virology

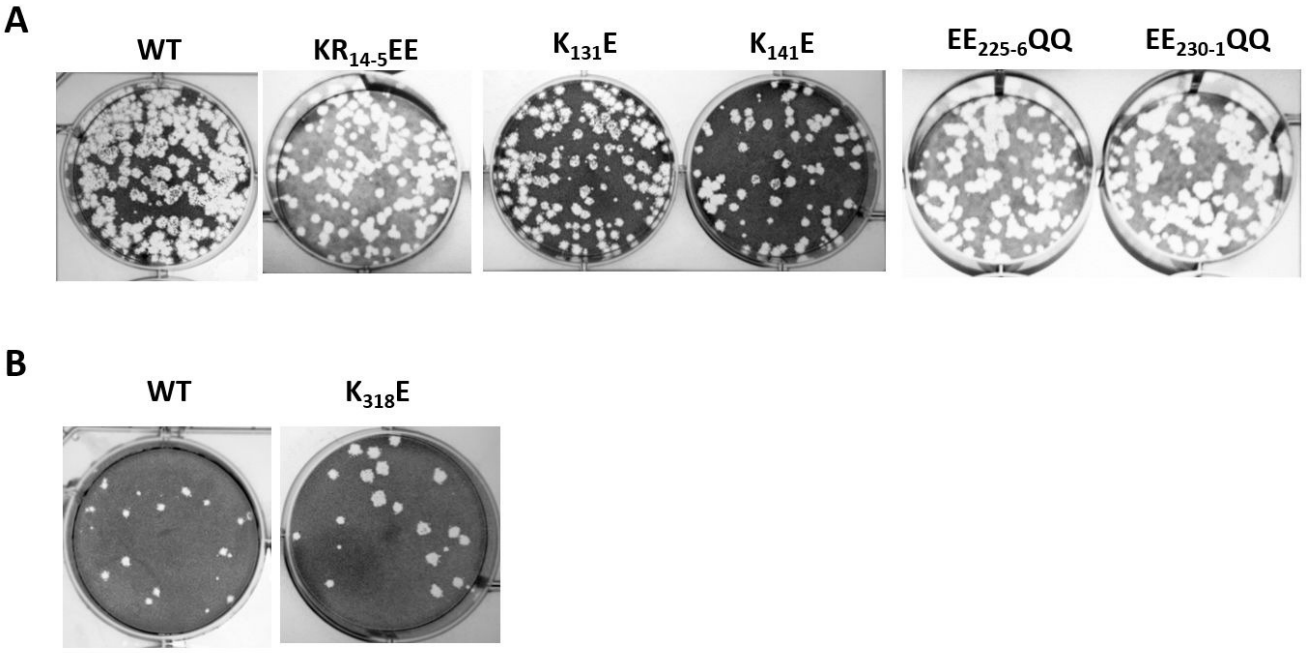

A

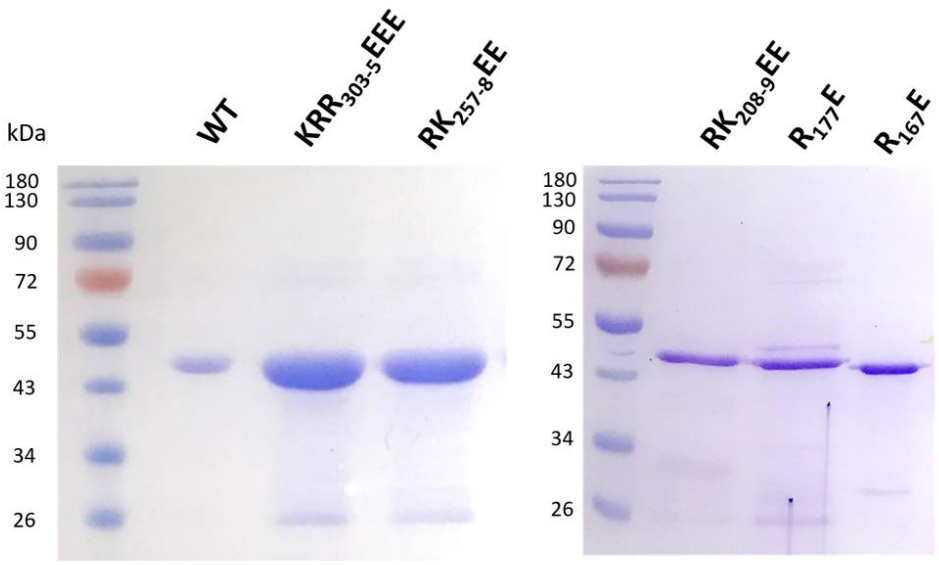

B

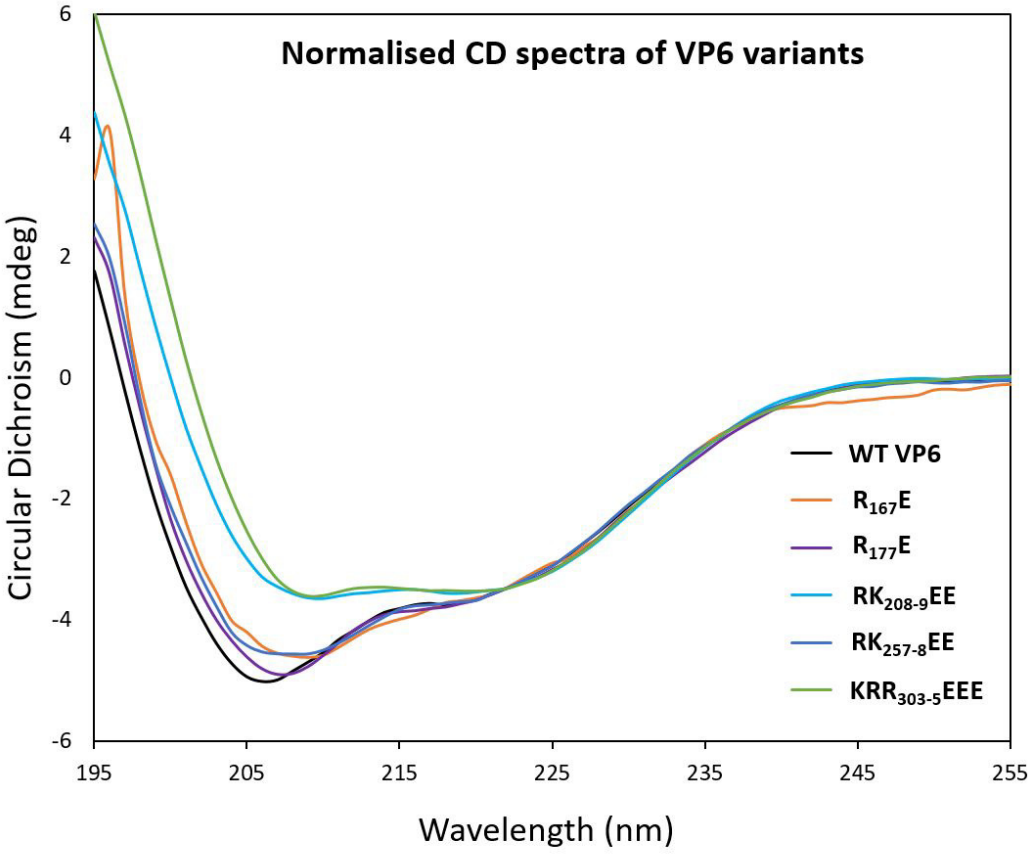

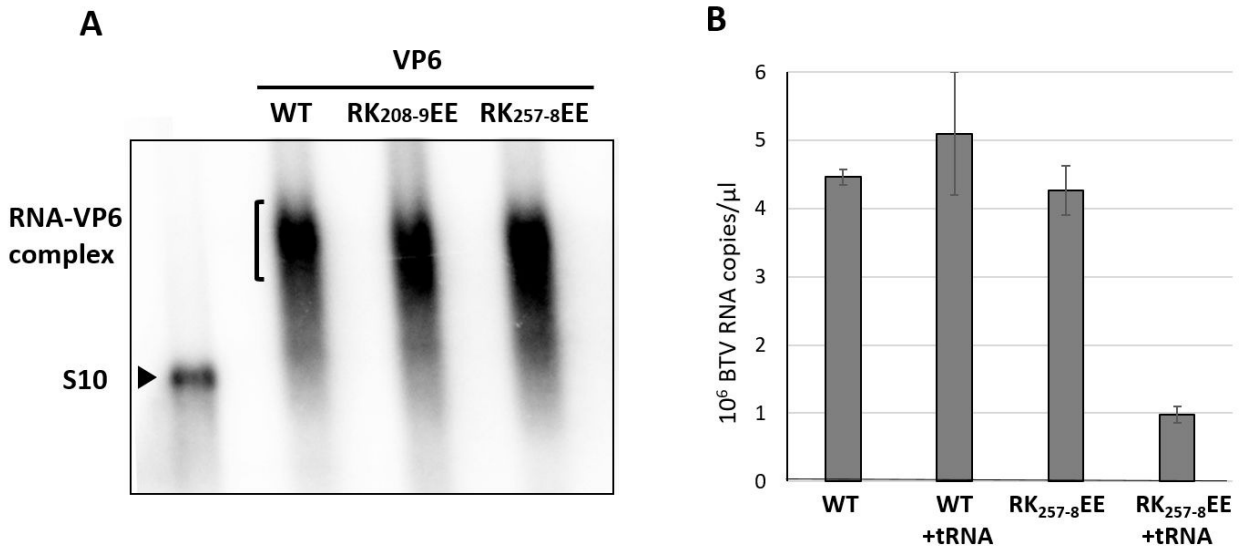

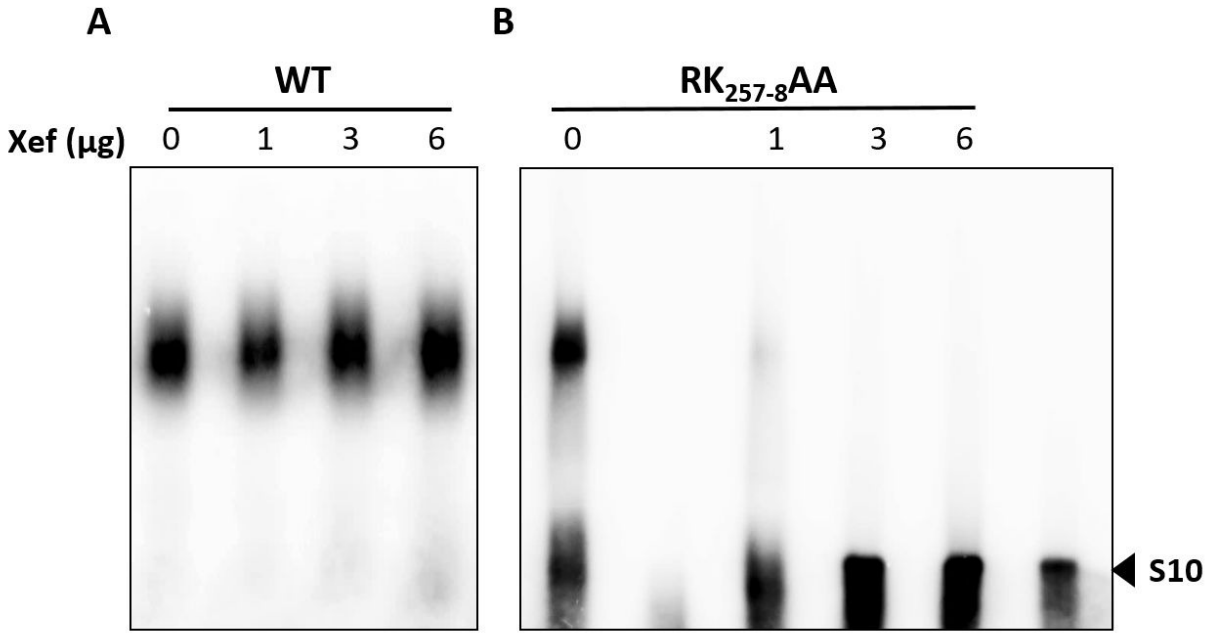

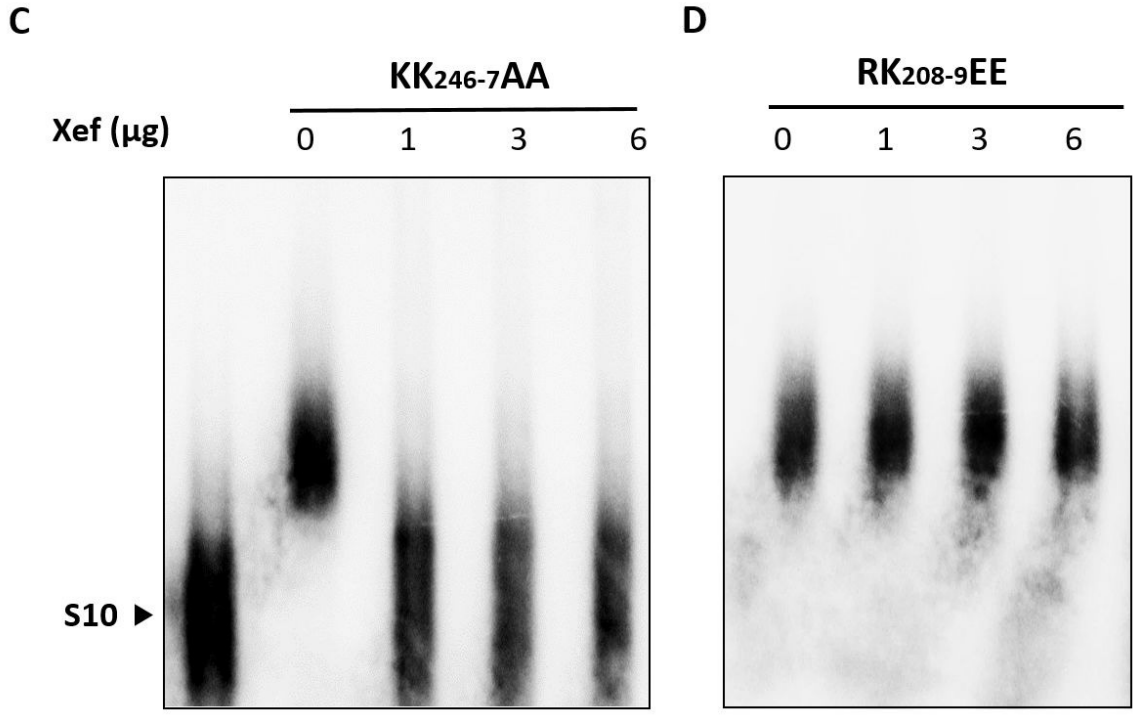

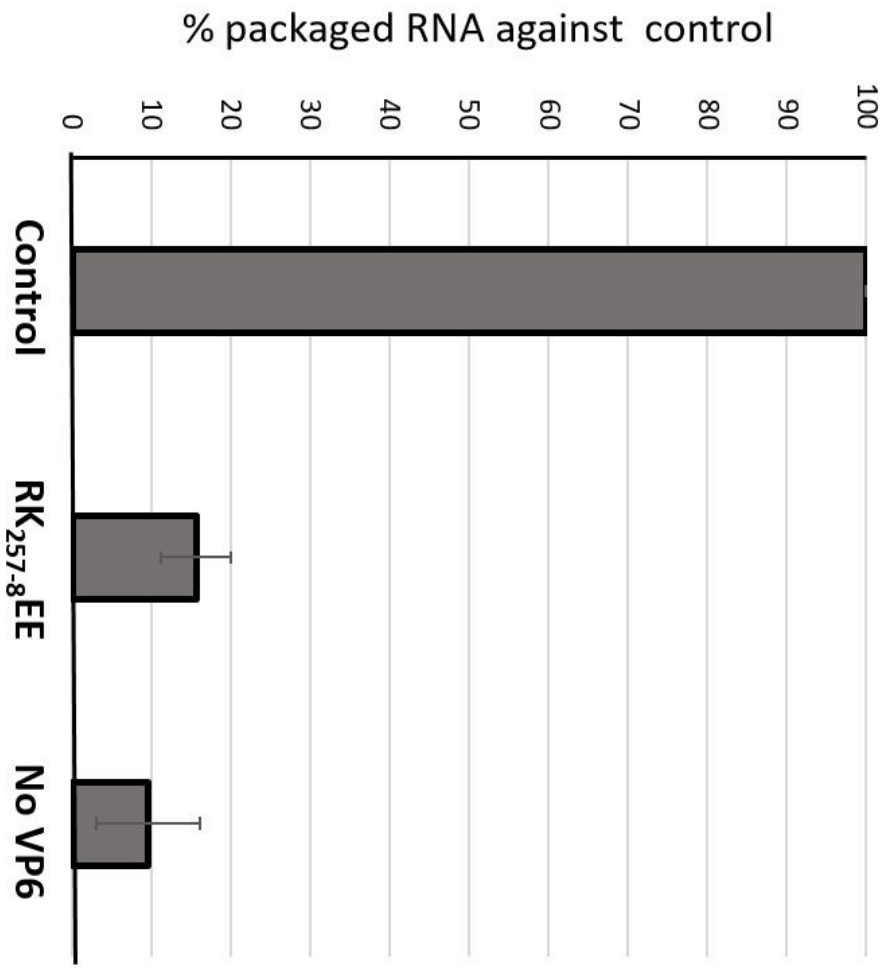

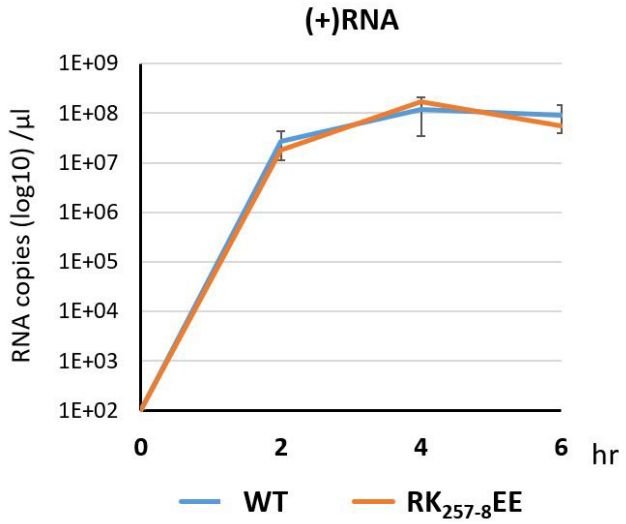

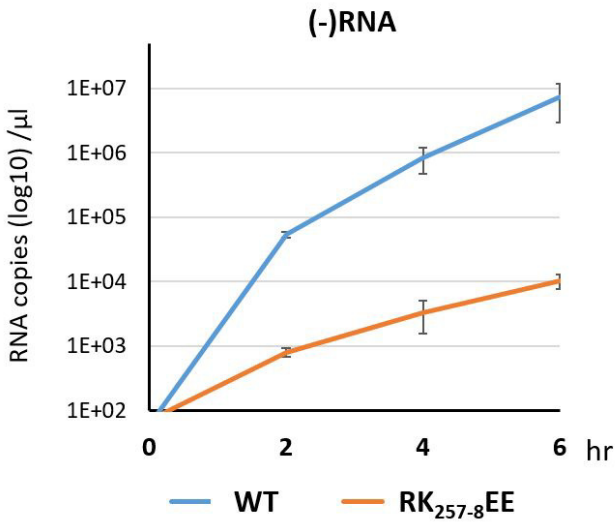

Table 1. Characteristics of the VP6 peptides assigned to contact RNA.

Sample	M/Z	Error (ppm)	Assign. Confid. (%)	Peptide sequence	AA #	Modifications	Fold above no HCHO
reVP6/ssRNA	655.39	4.7	97.8[&]	SAAILLAPGDVIK	2-14	Acetylation, N-term	>10*
reVP6/ssRNA	733.44	4.6	100	SAAILLAPGDVIKR	2-15	Acetylation, N-term	>10
reVP6/dsRNA	557.80	4.4	100	IHTAVGSGSGTK	83-94	None	>10
reVP6/ssRNA & reVP6/dsRNA	851.90	5.3	100	VGGGGGDADAGVGATGTNGGR	111-131	None	>10, 5.6
reVP6/ssRNA	608.34	0.5	100	WVVLTEEIAR	132-141	None	>10
Core/dsRNA	682.03	0.4	100	IDVYRDEVPAQIIEVER	151-167	None	>10
Core/dsRNA	789.68	2.4	100	IDVYRDEVPAQIIEVERSLQKELGISR	151-177	None	>10
Core/dsRNA	699.37	0.4	100	DEVPAQIIEVERSLQKELGISR	156-177	None	>10
reVP6/ssRNA & dsRNA	795.37	-3.6	100	EGVEEEKTSEEPAR	221-234	None	>10
reVP6/ssRNA & dsRNA	646.35	3.5	100	IGITIEGVMSQK	235-246	Oxidation of M9	>10
reVP6/ssRNA & dsRNA	545.80	1.6	100	GVMSQKKLLSMIGGVERKMA	241-260	Oxidation of M11	>10
reVP6/ssRNA, dsRNA, & Core	609.85	1.7	100	KLLSMIGGVER	247-257	Oxidation of M5	>10
reVP6/ssRNA & dsRNA	545.80	2.2	100	LLSMIGGVER	248-257	Oxidation of M4	5.2, 5.2
reVP6/ssRNA & dsRNA	647.34	1.3	100	ESAVMLVSNSIK	266-277	Oxidation of M5	>10
reVP6/ssRNA & dsRNA	588.32	1.5	100	ESAVMLVSNSIKDVVR	266-281	Oxidation of M5	>10
reVP6/ssRNA & dsRNA	554.94	-0.1	100	ATAYFTAPTGDPHWK	282-296	None	>10
Core/dsRNA	706.69	-1.6	83.9	ATAYFTAPTGDPHWKEVAR	282-300	None	>10
Core/dsRNA	669.85	0.1	100	NILAYTSTGGDVK	307-319	None	>10
Core/dsRNA	784.89	-0.8	100	NILAYTSTGGDVKTE	307-321	None	>10
Core/dsRNA	853.12	1.1	100	NILAYTSTGGDVKTEFLHLIDHL	307-329	None	>10
reVP6/ssRNA	473.94	4.5	100	IGITIEGVMSQKK	235-247	None	>10
reVP6/ssRNA	609.85	-2.6	82.9	LLSMIGGVERK	248-258	None	>10
reVP6/ssRNA	558.82	2.9	93.5	VSNSIKDVVR	272-281	None	>10

[&]Confidence of peptide assignment from collision-induced peptide fragmentation.

*The area of the peptide peak relative to the area in the reaction performed without formaldehyde.

Table 2. Conformational analysis of mutant reVP6.

VP6	Helix /loop (%) (α, π, 3,10 helix, loop)	Beta strands (%)	Turn (%)	RMSD
WT	48.0	36.6	15.5	0.0467
$R_{167}E$	47.7	37.0	15.3	0.0499
$R_{177}E$	47.3	37.1	15.5	0.0506
$RK_{208-9}EE$	47.4	37.2	15.5	0.0493
$RK_{257-8}EE$	47.8	36.8	15.4	0.0478
$KRR_{303-5}EEE$	47.3	37.3	15.4	0.0486